Report of Investigation 2022-5

COASTAL BLUFF STABILITY ASSESSMENT FOR HOMER, ALASKA

Richard M. Buzard and Jacquelyn R. Overbeck

Published by
STATE OF ALASKA
DEPARTMENT OF NATURAL RESOURCES
DIVISION OF GEOLOGICAL & GEOPHYSICAL SURVEYS
2022

Cover. Coastal bluff by the Sterling Highway, Homer, Alaska. Photo: Barrett Salisbury, Alaska Division of Geological & Geophysical Surveys.

COASTAL BLUFF STABILITY ASSESSMENT FOR HOMER, ALASKA

Richard M. Buzard and Jacquelyn R. Overbeck

Report of Investigation 2022-5

State of Alaska
Department of Natural Resources
Division of Geological & Geophysical Surveys

STATE OF ALASKA
Mike Dunleavy, Governor

DEPARTMENT OF NATURAL RESOURCES
Akis Gialopsos, Acting Commissioner

DIVISION OF GEOLOGICAL & GEOPHYSICAL SURVEYS
David L. LePain, State Geologist and Director

Publications produced by the Division of Geological & Geophysical Surveys (DGGS) are available for free download from the DGGS website (dggs.alaska.gov). Publications on hard-copy or digital media can be examined or purchased in the Fairbanks office:

Alaska Division of Geological & Geophysical Surveys
3354 College Rd., Fairbanks, Alaska 99709-3707
Phone: (907) 451-5010 Fax (907) 451-5050
dggspubs@alaska.gov | dggs.alaska.gov

DGGS publications are also available at:
Alaska State Library,
Historical Collections & Talking Book Center
395 Whittier Street
Juneau, Alaska 99811

Alaska Resource Library and Information Services (ARLIS)
3150 C Street, Suite 100
Anchorage, Alaska 99503

Suggested citation:
Buzard, R.M., and Overbeck, J.R., 2022, Coastal bluff stability assessment for Homer, Alaska: Alaska Division of Geological & Geophysical Surveys Report of Investigation 2022-5, 22 p., 2 sheets, scale 1:50,000.
https://doi.org/10.14509/30908

Contents

Figures

Tables

COASTAL BLUFF STABILITY ASSESSMENT FOR HOMER, ALASKA

Richard M. Buzard[1] and Jacquelyn R. Overbeck[1]

Abstract

We evaluate the stability of coastal bluffs in Homer, Alaska, using aerial imagery and modern elevation data. We produce maps of historical shoreline change and an alongshore bluff instability hazard score. Shoreline change is calculated by comparing the bluff top and toe positions in historical and modern orthorectified aerial imagery. Since 1951, Homer's coastal bluffs have eroded at an average rate of -1.0 ft/yr (-0.29 m/yr). Key indicators of bluff instability are historical shoreline change rates, bluff slope and height, vegetation, existing erosion protection structures, and water drainage. Most of the Homer coastline has a low to medium bluff instability hazard score. These coastal hazard assessment products can guide decisions to reduce risk.

INTRODUCTION

Coastal bluff failure poses a hazard to the City of Homer (Baird and Pegau, 2011; Kenai Peninsula Borough, 2019; Salisbury, in prep.). To assess this hazard, the Alaska Division of Geological & Geophysical Surveys (DGGS) created this report, associated maps, and GIS layers and data tables. This project is funded by the Federal Emergency Management Agency (FEMA) Cooperating Technical Partners (CTP) Program. This report is suitable to guide potential future updates to the FEMA Multi-Hazard Risk MAP analysis for Homer, and provide critical technical information for the next update of the Homer Local Hazard Mitigation Plan and future development plans or policies.

BACKGROUND

Geologic and Coastal Setting

The City of Homer, near the southwestern end of the Kenai Peninsula, is characterized by a prominent spit that extends into Kachemak Bay referred to locally as "Homer Spit" (Kenai Peninsula Borough, 2019; fig. 1). West of Homer Spit, bluffs near the coast rise to 800 ft (240 m) above mean sea level (MSL). The predominate rock type (the Kenai Group) comprises layers of poorly consolidated sands, silts, and clays, interbedded with medium- to low-grade coal (Barnes and Cobb, 1959). Coal beds dip less than 10 degrees away from the shoreline and act as aquicludes, resulting in perched water tables. The bluffs are partially vegetated with shrubs and trees. Exposed bluffs display visible groundwater seeps at coal beds. Properties at the top of the bluff overlook Kachemak Bay and Cook Inlet, with unimpeded views of the Kenai Mountains to the south and the volcanic Aleutian Range to the west. Coastal bluffs east of the spit are typically below 100 ft (30 m) above MSL and have numerous drainage channels. Residences and other infrastructure are built on the hilltops from Diamond Creek to past East End Road.

The majority of the Homer coastline consists of gently sloping (1 to 15 degrees) beaches of sand, pebbles, and cobbles (Kenai Peninsula Borough, 2021). Homer has semidiurnal tides with a great diurnal range of 18.4 ft (5.62 m; National Oceanic and Atmospheric Administration Center for Operational Oceanographic Products and Services [NOAA CO-OPS], 2020a; table 1). The local tidal datum was established in 2019, but the nearby Seldovia tide gage has been in operation since 1975 and has a similar datum (NOAA CO-OPS, 2020b; table 1). The highest water level recorded

[1]Alaska Division of Geological & Geophysical Surveys, 3354 College Rd., Fairbanks, Alaska 99709-3707.

in Seldovia reached 25.3 ft (7.72 m) above mean lower low water (MLLW) on November 5, 2002. Since 1964, relative sea level has fallen 1.8 ft (0.56 m; NOAA CO-OPS, 2020b).

Understanding Bluffs, Coastal Bluffs, and Erosion Rates

Bluffs are landforms that are steepened by erosion processes including wind, water, weathering,

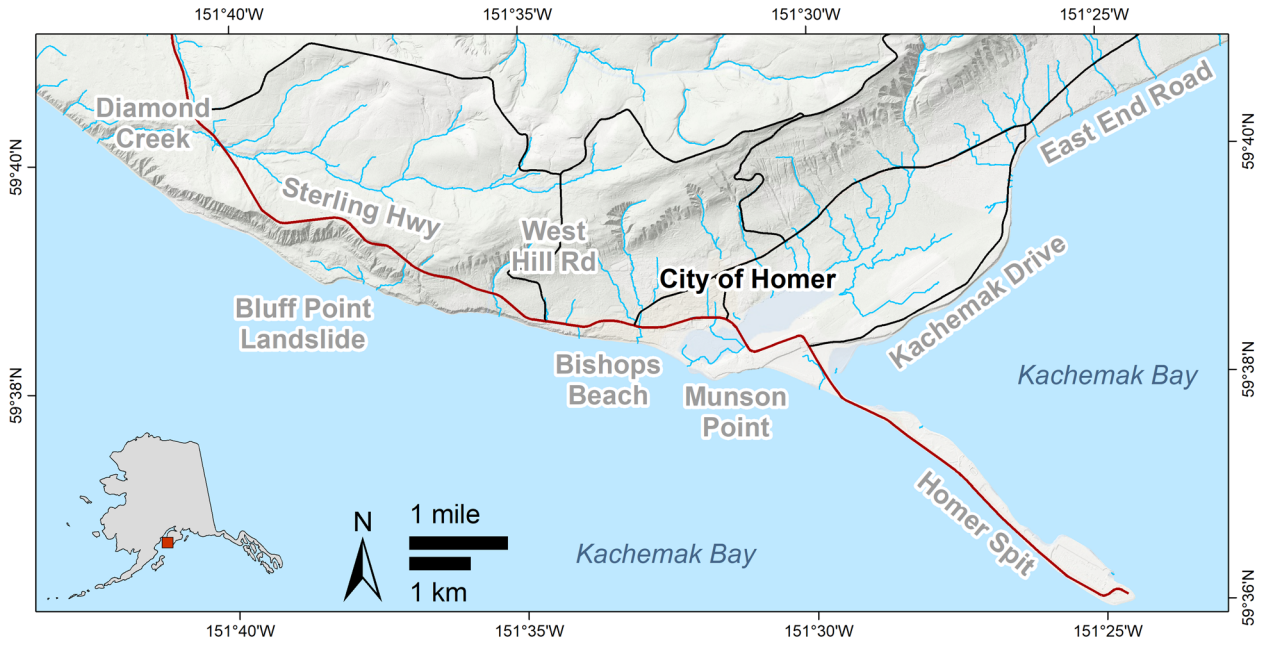

Figure 1. The area of interest for coastal bluff stability analysis includes the City of Homer and surrounding area. The hillshade elevation model shown was collected by Salisbury and others (2021).

Table 1. Tidal datums for Homer, Alaska (Coal Point; station 9455558), and nearby Seldovia (station 9455500).

Datum	Datum abbreviation	Homer ft (m) above MLLW	Seldovia ft (m) above MLLW
Mean Higher-High Water	MHHW	18.432 (5.618)	18.041 (5.499)
Mean High Water	MHW	17.592 (5.362)	17.231 (5.252)
Mean Tide Level	MTL	9.626 (2.934)	9.462 (2.884)
Mean Sea Level	MSL	9.734 (2.967)	9.554 (2.912)
Mean Diurnal Tide Level	DTL	9.216 (2.809)	9.091 (2.771)
Mean Low Water	MLW	1.657 (0.505)	1.696 (0.517)
Mean Lower-Low Water	MLLW	0.000 (0.000)	0.000 (0.000)
North American Vertical Datum of 1988	NAVD88	5.095 (1.553)	5.161 (1.573)
Great Diurnal Range	GT	18.432 (5.618)	17.231 (7.072)
Mean Range of Tide	MN	15.935 (4.857)	7.766 (6.308)
Highest Astronomical Tide	HAT	N/A	23.110 (7.042)

and tectonic motion. Bluffs and steep slopes are often the focus for hazard assessments because they can gradually or rapidly erode and have the potential for massive failure (Highland and Bobrowsky, 2008). Several factors can contribute to destabilize a slope, including earthquakes, undercutting, increased load (such as from groundwater or surface water flooding), stratigraphy and aquicludes, or weak vegetation (Hampton and Griggs, 2004; Highland and Bobrowsky, 2008; Kokutse and others, 2016).

There is not a quantitative definition for a coastal bluff. "Coastal bluff" is a general term to describe a steep slope that is eroded by coastal processes such as tides, waves, and currents (Hampton and Griggs, 2004). Coastal bluffs (and lake and riverine bluffs) can erode faster than inland bluffs due to frequent undercutting from water bodies. Coastal areas are also natural end points for watershed drainage, so ground and surface water accumulation may be higher than in inland areas (Heath, 1983).

Erosion of composite coastal bluffs (containing more than one type of material) commonly occurs in a two-step cycle of undercutting and steepening (toe erosion) via wave action, then mass movement (top erosion; Maine Geological Survey, 2015; fig. 2). The typical speed of this paired failure can dictate the proper method to assess a hazard: if there is annual to sub-decadal erosion, the hazard is described using long-term linear erosion rates (Himmelstoss and others, 2018). If erosion occurs rarely, such as on centennial or longer timescales, then it becomes more appropriate to describe hazards using probability or categorical hazard levels (such as Hapke and Plant, 2010). This is especially the case for extreme mass movements such as deep-seated landslides (Varnes, 1978; Salisbury, in prep.).

Coastal Bluff Erosion and Stability in Homer

The majority of Homer's coastline comprises bluffs. Using sets of aerial images from 1951 to 2003, Baird and Pegau (2011) calculate average erosion rates of 2.6 ft/yr (0.8 m/yr) west of the spit and 2.0 ft/yr (0.6 m/yr) east. The period of greatest erosion occurred after March 27, 1964, when the magnitude 9.2 Great Alaska earthquake caused an average 3.5 ft (1.1 m) of subsidence in the region (Stanley, 1968). High tide mostly submerged the spit, and waves reached the toes of many coastal bluffs (Gronewald and Duncan, 1965). Due to the unprecedented wave action, bluffs eroded as much as 8 ft (2.4 m) back in just 6 months (Stanley, 1968). Other than this major event, bluff erosion in Homer has been a slow process relative to many other Alaska communities (Overbeck and others, 2020). Still, several structures are near eroding bluffs and have potential to be exposed to erosion in the coming decades.

METHODS

This analysis focuses on two goals: (1) calculate historical bluff erosion, and (2) estimate current bluff stability. Historical bluff erosion is computed using orthorectified aerial imagery and the Digital Shoreline Analysis System (DSAS; Himmelstoss and others, 2018). Bluff stability is estimated by combining variables that factor into instability: height, slope angle, vegetation, drainage, erosion history, and shoreline armoring.

Lidar-derived elevation models are critical for this analysis. In 2019, DGGS collected lidar over Homer and created a bare earth digital terrain model (DTM) and digital surface model (DSM) with a ground sampling distance (GSD) of 1.6 ft (0.5 m; Salisbury and others, 2021; fig. 1). DGGS also collected oblique alongshore imagery. In the same year, the U.S. Army Corps of Engineers (USACE) collected topobathymetric lidar from the Homer spit northwest to Diamond Creek, creating a DTM with 3.3-ft (1.0 m) GSD (OCM Partners, 2021). USACE also created two orthomosaics (at high tide and low tide) with 2-inch (0.05 m) GSD.

Identifying Coastal Bluffs and Study Extent

The extent of the DGGS lidar is used as the study area boundary (fig. 1). All slopes with toes reaching a coastal area are examined for this study. We extract the Mean High Water (MHW) line (12.50

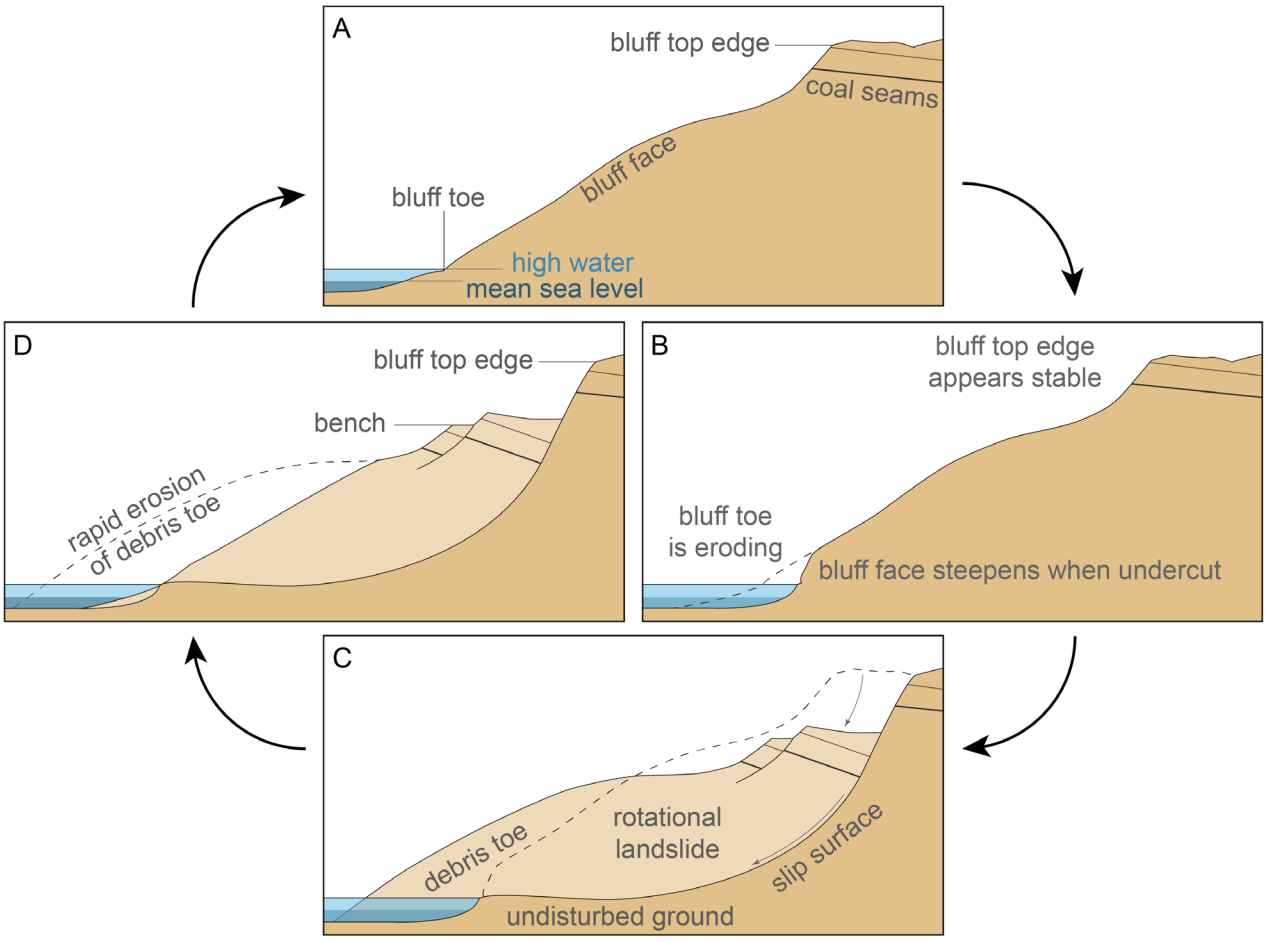

Figure 2. This schematic expands the two-step (top and toe) coastal bluff erosion cycle into four phases. **A.** The bluff is being eroded and undercut at the toe by storm-driven waves. **B.** Although the bluff top edge remains stable, the angle between the toe and top is steepening, leading to unstable conditions. **C.** A landslide (rotational slump) occurs and debris flows toward the ocean, lowering the blocks at the former bluff top edge along the slip surface. **D.** The debris in the intertidal and storm tide zone is eroded relatively quickly. Erosion slows because the remaining bluff is outside the intertidal zone. The new bluff face is at a shallower angle than before, and the cycle renews.

ft [3.809 m] NAVD88) using the DGGS DTM and smooth it to contour the coastline. Along this line, we delineate the 2019 bluff toe and top using a combination of digital elevation models (DEM), orthomosaics, and oblique aerial imagery. The toe is generally defined as the seaward extent of a slope where (1) a break to relatively flat land occurs (often a sediment transition), (2) land continues down to the MHW line, and (3) there exists along the transect no topography higher than the bluff toe (fig. 3). The bluff top edge is identified as the seaward extent of relatively flat land where a slope break or scarp occurs. For complex slopes with benches, the bluff top edge is landward of the benches (fig. 3). These manually delineated bluff features define the envelope where bluff face characteristics are measured.

Historical Shoreline Change Analysis

Traditionally, shoreline change is calculated by matching two aerial images taken at different times, delineating shorelines, and measuring the distance between them (Baird and Pegau, 2011; Overbeck and others, 2020). The coastal bluff erosion history in Homer has been calculated many times using this method, as recently as 2016 (City of Homer, 2021). We received the shorelines and imagery from 1951 to 2003 that were used and found two major

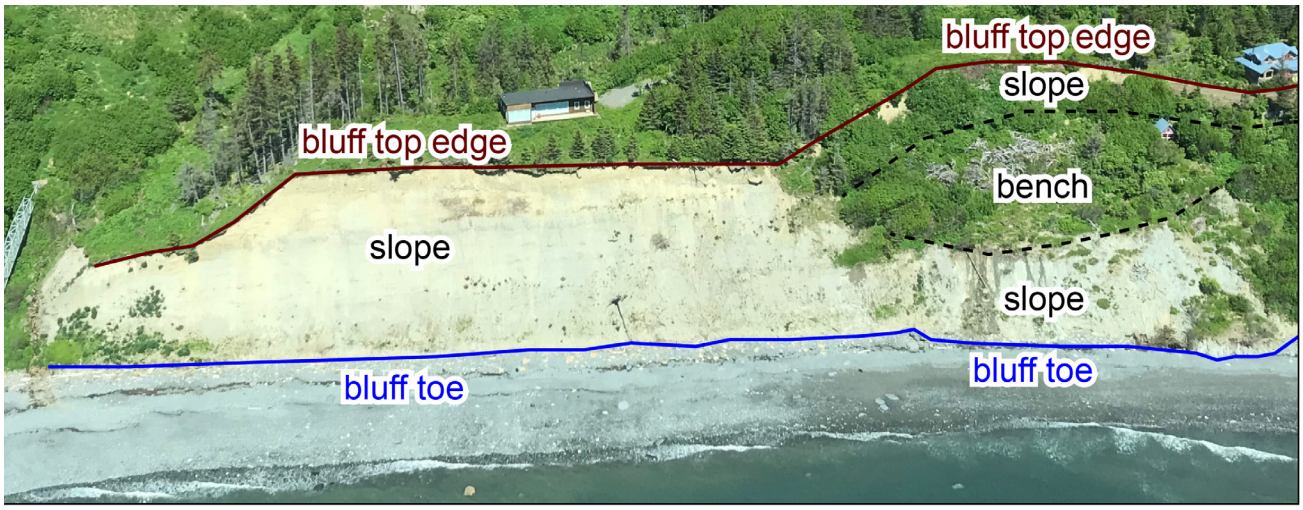

Figure 3. Oblique image of a coastal bluff with delineated toe (blue) and top edge (maroon). The right side shows how delineations are made for a complex section. The bluff has a bench (black dashed lines), so the delineated top edge is landward of this bench. In this example, there is a building on the bench that is seaward of the bluff top edge (far right side).

components that have caused significant errors: (1) some of the image sets are not orthorectified, and (2) delineations do not consistently follow the same features through time in all areas (switching between bluff top and toe). The affected images and shorelines are for the years 1951, 1961, 1968, 1975, and 1996. The orthorectified 2003 image is adequate. For these reasons, we source raw aerial imagery to orthorectify, delineate shorelines, and compute shoreline change using the DSAS tool (Himmelstoss and others, 2018). The orthoimagery dates are 1951/1952, 1964, 1985, 2003, 2011, and 2019 (table 2). The time steps between image collections are 12 or 13, 21, 18, 8, and 8 years, respectively.

Image Corrections

Orthometric corrections are vital for evaluating erosion of tall, steep bluffs. Buzard (2021) explains the historical aerial image orthorectification process. Historical aerial photos are initially collected with a low distortion frame lens pointed at nadir. A simple method to display these images in a map is to shift and scale them to match features on the landscape. This method, called "georeferencing" or "georectification," may appear adequate from a distance, but the perspective from the image center causes offsets at finer scales (termed "relief displacement;" Crowell and others, 1991). Offsets increase near high-angle features, such as bluffs, and cause

Table 2. Imagery used for shoreline delineations include color (RGB), color-infrared (CIR), and black and white (BW).

Date	Type	Orthomosaic pixel size (m)	Source
2019 JUL 17	RGB	0.05	OCM Partners (2021)
2011	RGB	0.75	GeoNorth Best Data Layer (Best Data Layer)*
2003	RGB	1.00	Baird and Pegau (2011)
1985 AUG 27	CIR	1.88	NASA AMES Research Center
1964 APR 14	BW	0.55	U.S. Army Corps of Engineers
1951/1952	BW	1.14	U.S. Air Force

* hub.arcgis.com/documents/ADEC::alaska-geospatial-council-agc-imagery-services/about

significant inaccuracy to bluff delineations. To allow for accurate measurements across the horizontal geographic plane on the image, the image must be orthorectified. Orthorectification is the process by which the perspective of an entire image is corrected to nadir: anywhere one looks in the orthorectified aerial image will appear as if looking straight down. Orthorectification can be accomplished using a DEM acquired near the same time as the image, or by using performing photogrammetric (or structure-from-motion) techniques on a collection of overlapping images. An orthorectified product is called an orthoimage or orthomosaic.

Shoreline Change Rate Calculations

The USGS created the DSAS tool to compute shoreline change by casting virtual transects perpendicular to an alongshore baseline and measuring the distance between shorelines on each transect (Himmelstoss and others, 2018). We space transects 16.4 ft (5 m) apart and calculate shoreline change rates separately for the bluff top edge and bluff toe. The average of these rates is used for the final change rate. This method summarizes total bluff erosion and is less susceptible to episodic events related to the bluff erosion cycle (Buzard and others, 2020). Where at least three shorelines are present, we calculate the weighted linear regression rate of change (WLR) and associated 90 percent confidence interval (WCI90). Otherwise, the end point rate of change (EPR) is calculated. These metrics describe the long-term erosion trend using an annualized linear rate of change in distance per year.

Shoreline Delineation

We delineate the bluff top and toe in each orthoimage. Slow and episodic bluff erosion complicates shoreline erosion calculations that rely on only one feature. For example, if the bluff toe eroded between two images and a study only calculates bluff top change, the study will incorrectly identify that bluff as stable when it is steepening and getting closer to a mass movement. Likewise, if a mass movement did occur over the study period, the bluff top edge may suggest far faster rates of erosion than will be seen in the future. Tracking the top and toe can determine what stage of the erosion cycle a bluff is in and improve understanding of current erosion hazards.

Bluff toes are generally clearly identifiable as the seaward extent of a slope. Bluff tops are more subjective because some areas have partial slides or benches, leading to multiple edges. The chosen bluff top edge must represent the seaward extent of land that is neither part of a previous landslide nor a bench on a slope (fig. 3). We refer to the 2019 lidar to ensure the correct bluff top edge is chosen, but only use imagery for these delineations to maintain consistency. Interpretations of historical aerial imagery are aided by the DSMs produced by the orthorectification process. Where vegetation made visual interpretation challenging, a slope map is used to identify steep slope breaks (fig. 4). This method helps to maintain consistent tracking of the bluff top edge and toe, especially

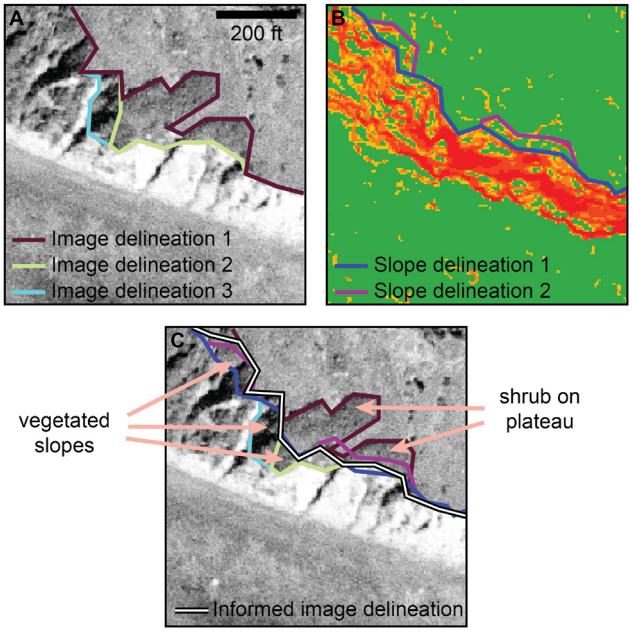

Figure 4. Slope maps generated from DSMs were used to help identify slope breaks obscured by vegetation. **A.** The orthoimage in 1951 has vegetation growing down the slope, making the bluff top edge challenging to identify. The three colored lines are separate interpretations of where the bluff top edge could be. **B.** The steep slope map is derived from the digital surface model created during the orthorectification process. The bluff top edge and toe are close to where steep slope angles (red) meet shallow slopes (green). **C.** A new delineation is made on the orthoimage, assisted by the interpretations from the slope map.

around benches and complex bluffs. The shoreline delineations are still made using the orthoimage.

This study has one digitizer. Digitizing precision uncertainty represents the consistency with which the digitizer can interpret and trace a feature in an image. To compute digitizing precision, sections of the bluff toe totaling 3.3 miles (5.3 km) in length are delineated three times on the GeoNorth Best Data Layer (BDL; hub.arcgis.com/documents/ADEC::alaska-geospatial-council-agc-imagery-services/about. We cast transects at 16.4-ft (5 m) spacing perpendicular to these lines to measure the distance between them. Digitizing precision (U_d) is calculated by taking the mean of the maximum distance between the three lines (L_1, L_2, L_3) on each transect (equation 1).

Equation 1:

$$U_d = \sum_{i=1}^{n} \frac{max\left(|L_{1i} - L_{2i}|, |L_{1i} - L_{3i}|, |L_{2i} - L_{3i}|\right)}{n}$$

U_d = digitizer uncertainty

L_n = distance to baseline

The total uncertainty (U_t; equation 2) represents the positional accuracy of the delineated shorelines relative to real-world coordinates (table 3). Total uncertainty is high because all images are referenced to the BDL that has a total horizontal uncertainty of 6.3 ft (1.92 m). The total uncertainty relative to the BDL (U_r; equation 3) represents the positional accuracy of delineated shorelines relative to each other (table 4). This is a more appropriate metric for estimating uncertainty of delineations on imagery that are referenced relative to the same image.

Equation 2:

$$U_t = \sqrt{U_o^2 + U_p^2 + U_d^2}$$

Equation 3:

$$U_r = \sqrt{U_i^2 + U_p^2 + U_d^2}$$

U_t = total uncertainty of shoreline delineation

U_o = total uncertainty of image

U_r = relative uncertainty of shoreline delineation

U_t = relative uncertainty of image

U_p = pixel size

Coastal Bluff Stability Assessment

Long-term, annualized erosion rates may not adequately identify potential instability. We assess current coastal bluff stability by identifying combinations of variables that contribute to instability (similar to Maine Geological Survey, 2015). The chosen variables are erosion rate, slope angle, vegetation, water drainage, and erosion mitigation (fig. 5). (See "Study Limitations" for a discussion

Table 3. Total uncertainty of image orthorectification (U_o) and shoreline delineation (U_t). All values are in meters.

Year	Total uncertainty	Pixel size	Uncertainty to control	Uncertainty to BDL	Total image uncertainty	Digitizer uncertainty
	U_t	U_p	$U_{o,source}$	U_i	U_o	U_d
2019	**1.06**	0.05	0.07	1.92	0.07	1.06
2011	**2.32**	0.75	1.92	-	1.92	1.06
2003	**3.61**	1.00	1.92	2.69	3.30	1.06
1985	**4.20**	1.88	1.92	3.05	3.60	1.06
1964	**2.43**	0.55	1.92	0.89	2.12	1.06
1951/1952	**3.65**	1.14	1.92	2.68	3.30	1.06

Table 4. Relative total uncertainty of shoreline delineation (U_t). All values are in meters.

Year	Total uncertainty	Pixel size	Uncertainty to BDL	Digitizer uncertainty
	U_t	U_p	U_i	U_d
2019	**2.19**	0.05	1.92	1.06
2011	**1.30**	0.75	-	1.06
2003	**3.06**	1.00	2.69	1.06
1985	**3.74**	1.88	3.05	1.06
1964	**1.49**	0.55	0.89	1.06
1951/1952	**3.10**	1.14	2.68	1.06

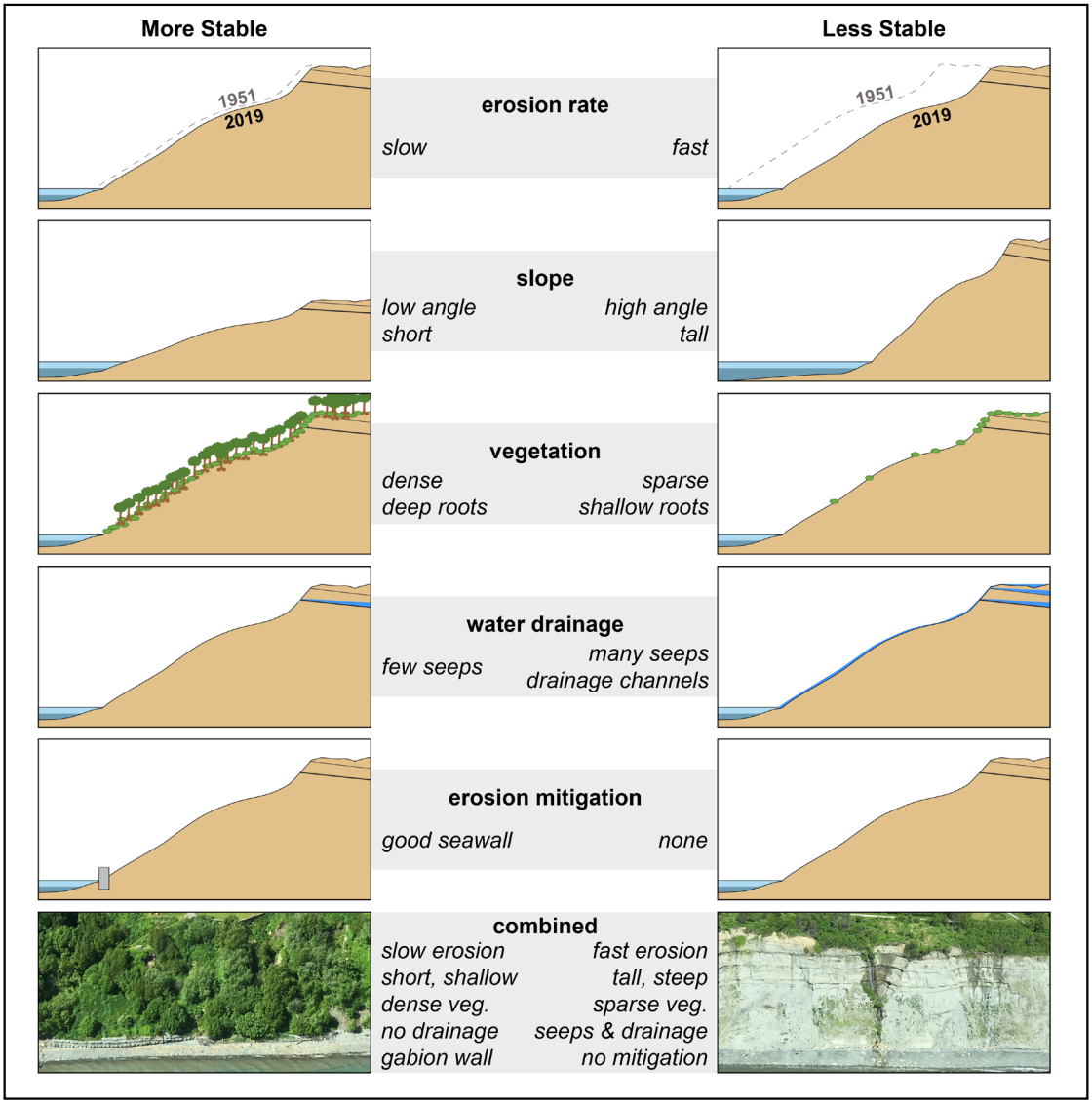

Figure 5. Conceptual diagram of bluff instability variables. The combination of variables determines the overall stability.

about these and other possible variables.) Each variable is evaluated using four instability categories: very low, low, medium, and high. The categories are combined for a total instability hazard score (fig. 5). Coastal slopes are manually identified using the delineations of the bluff top and toe from the DGGS DTM. Transects are cast perpendicular to the bluff toe at 16.4-ft (5-m) spacing along 14 miles (22 km) of shoreline. Variables are computed along each transect.

Instability Due to Erosion Rate

Coastal zone management often uses linear regression erosion rates to define coastal setback zones and erosion hazard areas (Crowell and others, 2018; Perello, 2019). We multiply the average erosion rate of the bluff top and toe by 50 years to extrapolate possible future erosion distance based on observed change over the past 60 to 70 years. Fifty years is chosen because structures are commonly designed with 50-year design life (Val and others, 2019). Instability categories are based on coastal setback values of 15 and 40 ft (4.6 and 12 m; table 5). These setback distances are commonly used by homeowners or builders in Homer in compliance with existing city zoning. For example, if erosion rates suggest between 15 and 40 ft (4.6 and 12 m) of erosion will occur in the next 50 years, the location has a medium instability score in the erosion category.

Instability Due to Slope and Height

Greater slope angle increases the probability of a mass movement occurring (Highland and Bobrowsky, 2008; Kokutse and others, 2016). We use factor of safety (FOS) results to determine safe and unsafe slope angles. Salisbury (in prep.) calculates that, in Homer, silty sand slopes below 27 degrees tend to have an FOS greater than 1.5, meaning they have lower likelihood of failure. Kokutse and others (2016) find a similar slope angle threshold of 27 degrees for sand, silt, and clay slopes. Rotational landslides are common modes of mass movement in Homer (Reger, 1979; Berg, 2009), so we use this as the failure type. We assume any slope greater than 27 degrees has some likelihood of failure, and if it fails in a rotational landslide the post-movement slope will be 27 degrees (51 percent slope) hinging roughly about the toe (Bishop, 1955; Chowdhury and Xu, 1994; Jiang and others, 2017; fig. 6). On each profile, we calculate the slope percent from toe to top (B_s) and subtract 51 percent slope to determine the angle change (equation 4).

In the context of hazards to infrastructure on the bluff, the greatest concern is the inland distance that the mass movement head scarp will reach. The erosion distance (B_e) is proportional to the height

Table 5. Instability category thresholds for 50 years of bluff erosion (E_{50}) based on historical erosion rates.

Instability category	Erosion distance (ft)
High	$E_{50} > 40$
Medium	$15 < E_{50} \leq 40$
Low	$0 < E_{50} \leq 15$
Very low	$E_{50} = 0$

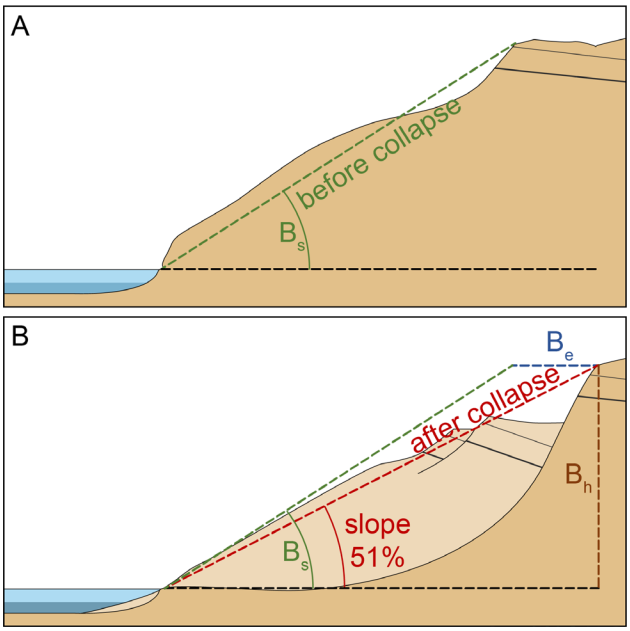

Figure 6. A. The current slope angle between the top and toe (B_S) is reduced after a mass movement **B.** Bluff erosion (B_e) is a function of height (B_h) and change from B_S to 51 slope percent. Taller and steeper bluffs experience greater horizontal erosion.

(B_h) and the change in slope (Bishop, 1955; fig. 6, equation 4). Instability categories are based on coastal setback values of 15 and 40 ft (4.6 and 12 m; table 6).

Equation 4:

$$B_e = B_h \times (B_s - 0.51)$$

B_e = horizontal bluff erosion due to slope failure

B_h = bluff height

B_s = average bluff slope percent (as a fraction)

Table 6. Instability category thresholds for bluff erosion (B_e) due to slope failure.

Instability category	Erosion distance (ft)
High	$B_e > 40$
Medium	$15 < B_e \leq 40$
Low	$0 < B_e \leq 15$
Very low	$B_e = 0$

Instability Due to Lack of Vegetation

Exposed slopes are often used as a proxy for instability because they can imply recent failure and/or frequent erosion (Salisbury, in prep.). Deforestation is commonly a contributing factor to landslides (Highland and Bobrowsky, 2008). Vegetation improves slope stability primarily through soil cohesion via root tensile strength and reduced soil moisture via evapotranspiration and reduced infiltration (Wu, 1984). Vegetation also reduces erosion from wind and surface runoff. Kokutse and others (2016) show that the FOS of non-reinforced slopes is increased by up to 19 percent by trees, 14 percent by shrubs, and 7 percent by grasses. This increase is due to the root matrix increasing soil cohesion. However, heavy precipitation can increase sediment pore pressure, reduce the tensile strength of roots, and increase surface load, leading to shallow landslides (Hales and Miniat, 2017). The increased surcharge from trees can improve stability, except on very steep slopes (Nilaweera and Nutalaya, 1999; Kokutse and others, 2016). Despite these scenarios, increased vegetation is considered a net-positive for slope stability (Wu, 1984).

The root properties influencing soil cohesion are roughly proportional to vegetation height (Kokutse and others, 2016). We quantify the instability due to lack of vegetation using a function of vegetation height and coverage, similar to Maine Geological Survey (2015; table 7). On slope profiles, we calculate vegetation height as the difference between the DGGS DSM and DTM. We use mean vegetation height on each profile to generalize the type (grass, shrub, and tree). In Alaska, vegetation is classified as a small tree when it reaches 12 ft (4 m) in height (among other variables related to canopy and trunk width; Little, 1953). However, willow—a large shrub common to Homer (Ager, 1998)—is considered a tree due to its size and likeness to trees (Viereck and Little, 1972). Therefore, we consider vegetation height exceeding 5 ft (1.5 m) to be trees and large shrubs (Viereck and Little, 1972). Per Viereck and Little (1972), we classify heights below 2 ft (0.6 m) as grasses and small shrubs. While the average vegetation height calculation includes the entire profile, we had to limit percent coverage to vegetation at or above 3.3 ft (1.0 m; medium shrub) to reduce overestimations due to DEM noise.

Instability Due to Lack of Erosion Protection

Existing erosion protection structures can reduce erosion rates and prevent undercutting of

Table 7. Instability category thresholds for vegetation type and coverage. The final category is the average of vegetation and coverage, rounding towards the least stable condition. For example, a slope with trees (low) and 25 to 49 percent coverage (medium) is in the medium category. A slope with shrubs (medium) and greater than 75 percent coverage (very low) is in the low category.

Instability category	Vegetation type and coverage
High	Grass or less than 25 percent coverage
Medium	Shrubs or 25 to 49 percent coverage
Low	Trees or 50 to 75 percent coverage
Very low	Trees and greater than 75 percent coverage

coastal bluffs. Complex engineered structures such as seawalls and gabions tend to prevent erosion better than simple structures such as riprap or piled debris (USACE, 2004; Rella and Miller, 2012). During the 2019 lidar survey, DGGS also collected alongshore oblique aerial imagery. We orthorectify and roughly georeference these data to create high-resolution 3D models in Agisoft Metashape. Using these models and other imagery, we delineate lengths of shoreline armoring and give a qualitative score of their current condition (The criteria are based on the observed condition of the structure. Good: little to no signs of degradation or movement. Fair: some signs of degradation, movement, or leaning but structure appears to function as intended. Poor: structure has moved or broken in places that impair the intended function.). Instability is categorized as a function of armoring type and current condition (table 8). Erosion protection structures can have significant detrimental effects, especially to natural sediment dynamics and beach nourishment (Ruggiero, 2010). We include existing erosion protection because it is an important factor for assessing current instability. We do not express or imply whether existing or new structures are appropriate solutions for bluff instability hazards.

Table 8. Instability category thresholds for erosion protection.

Instability category	Erosion protection condition and type
High	None, or poor riprap
Medium	Poor seawall/gabion, fair riprap
Low	Fair seawall/gabion, good riprap
Very low	Good seawall/gabion

Instability Due to Drainage

Precipitation, groundwater, and streams lead to slope instability. Surface runoff causes erosion, confining layers cause perched water tables, and increased pore fluid pressure reduces soil cohesion (Harp and others, 2006; Bukojemsky and Scheer, 2007). The water table generally mirrors surface topography, and lakes and streams are surface expressions of the water table (Heath, 1983; Winter and others, 1998). We follow the assumption that areas where water collects have more groundwater flow and greater potential for related hazards.

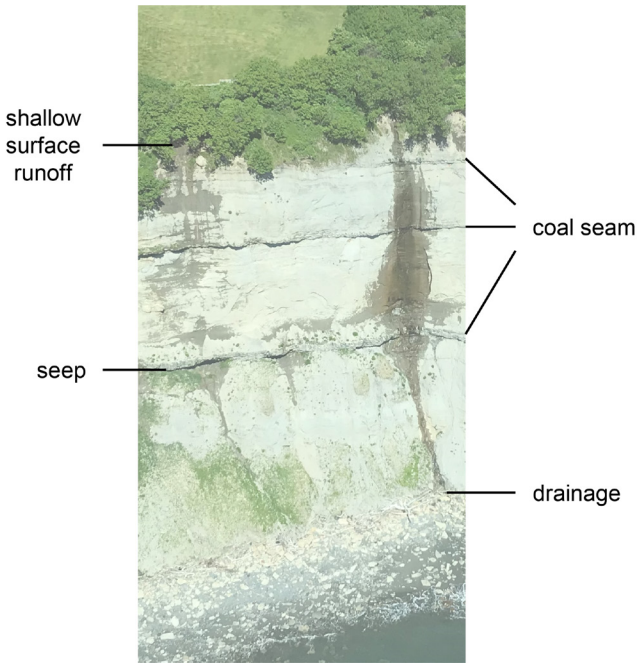

Figure 7. This 200-ft coastal bluff in Homer has surface runoff causing a continuous stream that drains to the beach. Groundwater also seeps from coal seams and other changes in the stratigraphy. Water causes channeling on the bluff face and undercuts coal seams, leading to instability.

We identify surface and groundwater expressions on the bluff slope using 3D models and imagery (fig. 7). However, many areas are obscured by vegetation, so water expressions may not be visible. In addition, the imagery only provides a snapshot in time, and conditions may have been unseasonably wet or dry. To consistently map drainage, we correlate observed hydrologic features with the flow accumulation through each transect based on the DTM. Flow accumulation represents the area of contributing streams toward a single point on the land surface within a user-defined catchment area. We identify flow channels on the DGGS DTM, correct the DTM to allow for flow through culverts under roads, then calculate the direction and accumulation of flow using ArcGIS hydrology tools. We correlate maximum flow accumulation and visible water expressions on each transect.

Shallow surface runoff and groundwater seeps tend to have lower flow accumulation than visible drainage streams and creeks. Half of all shallow surface runoff zones and seeps have flow accumulation below 27,000 ft^2 (2,500 m^2), so this is used as a lower cutoff to identify areas of very low drainage. As flow accumulation increases to 200,000 ft^2 (18,500 m^2), surface runoff and seeps transition to visible drainage channels. This is used as the lower threshold for medium drainage (where running water is actively causing minor erosion). Well-developed surface drainage channels primarily have flow accumulation upward of 540,000 ft^2 (50,000 m^2), and transition to creeks as flow increases. This flow accumulation value is used for the high drainage category (table 9). The value's magnitude is somewhat arbitrary because it is limited by the user-defined catchment; hence, we correlate the relative magnitude with observed hydrologic conditions.

Table 9. Instability category thresholds for drainage.

Instability category	Drainage indicators
High	Creeks, streams, continuous flow of water causing erosion
Medium	Flow of water from seeps and runoff causing minor erosion channels on bluff and beach
Low	Seeps and runoff exist but are not causing beach erosion
Very low	Seeps and runoff are rarely present

Combining Instability Variables

Instability variables are combined into one metric to determine the hazard posed by a combination of factors that destabilize slopes. No two categories are strongly correlated (table 10). Weights are not applied, but we give special consideration for areas with coastal armoring. Like vegetation, armoring can stabilize slopes and prevent erosion (Rella and Miller, 2012). For this reason, we use the most stable score between vegetation and armoring. For example, a seawall in good condition with no vegetation scores "very low" in the vegetation category. Similarly, we adjust the erosion score to the lesser of erosion and armor. This adjustment means an area with historically rapid erosion still scores "very low" if a seawall in good condition now exists. If an area has no armoring but very slow erosion, it still scores "very low." These modifications are only applied to the calculation of combined instability hazard scores; the original individual values are still available in the geodatabase. After these adjustments, combined instability is calculated using the average score rounded to the less stable score. The

Table 10. Correlation between instability variables. Values closer to 1 are strongly positively correlated (as variable 1 increases, variable 2 increases). Values of 0 are not correlated. Values closer to -1 are strongly negatively correlated (as variable 1 increases, variable 2 decreases).

	Armoring	Erosion	Slope	Vegetation	Drainage	Combined
Armoring	1					
Erosion	0.02	1				
Slope	0.19	0.08	1			
Vegetation	-0.17	0.42	0.26	1		
Drainage	0.12	-0.04	-0.18	-0.18	1	
Combined	0.41	0.56	0.52	0.54	0.21	1

average calculation involves four category values: drainage, slope and height, the most stable score between vegetation and armoring, and the most stable score between erosion and armoring.

RESULTS

Coastal bluff hazards are assessed using a historical shoreline change analysis and by combining bluff instability variables into a categorical hazard map. The shoreline change maps are more representative of the effects of long-term erosion trends. The bluff stability map communicates the potential for slope failure that may not be reflected in the historical erosion record.

Historical Shoreline Change Analysis (Map Sheet 1: Shoreline Change [1951 to 2019])

Shoreline change rates are between 1.0 and -3.9 ft/yr (0.3 and -1.2 m/yr; tables 11, 12). Erosion rates are greatest around the Bluff Point landslide

Table 11. Coastal bluff characteristics by region in feet and slope percent. Mean values are in bold type. Bluff height is the difference between the top and toe elevation. Slope angle is between the bluff top and toe. Slope angle standard deviation (SD) is shown as a range about the mean because slope percent does not scale linearly with degrees. Negative shoreline change is erosion, positive is seaward movement of the shoreline (such as by accretion, aggradation, or mass movements).

	Bluff Height (ft)				Slope Angle (percent)				Shoreline Change Rate (ft/yr)			
	Mean	SD	Min.	Max.	Mean	Mean ± SD	Min.	Max.	Mean	SD	Min.	Max.
Diamond Crk	**310**	82	186	473	**31**	23 to 39	18	51	**-0.5**	0.3	-1.2	0.3
Bluff Pt	**79**	53	17	485	**74**	41 to 121	17	184	**-1.7**	1.0	-3.7	0.8
Downtown	**139**	75	12	276	**87**	39 to 179	22	205	**-1.0**	0.5	-2.7	0.7
Munson Pt	**16**	5	1	28	**64**	40 to 94	12	114	**-0.8**	1.3	-3.9	0.8
Kachemak Dr	**55**	23	10	89	**73**	44 to 113	24	317	**-0.5**	0.6	-2.7	0.7
East End Rd	**68**	16	26	113	**56**	31 to 87	17	128	**-1.1**	0.4	-3.2	0.7

Table 12. Coastal bluff characteristics in meters and degrees.

	Bluff Height (m)				Slope Angle (degrees)				Shoreline Change Rate (m/yr)			
	Mean	SD	Min.	Max.	Mean	SD	Min.	Max.	Mean	SD	Min.	Max.
Diamond Crk	**94**	25	57	144	**17**	4	10	27	**-0.15**	0.09	-0.37	0.09
Bluff Pt	**24**	16	5	148	**37**	14	10	61	**-0.52**	0.30	-1.13	0.24
Downtown	**42**	23	4	84	**41**	20	12	64	**-0.30**	0.15	-0.82	0.21
Munson Pt	**5**	2	0	9	**33**	11	7	49	**-0.24**	0.40	-1.19	0.24
Kachemak Dr	**17**	7	3	27	**36**	12	13	72	**-0.15**	0.18	-0.82	0.21
East End Rd	**21**	5	8	34	**29**	12	10	52	**-0.34**	0.12	-0.98	0.21

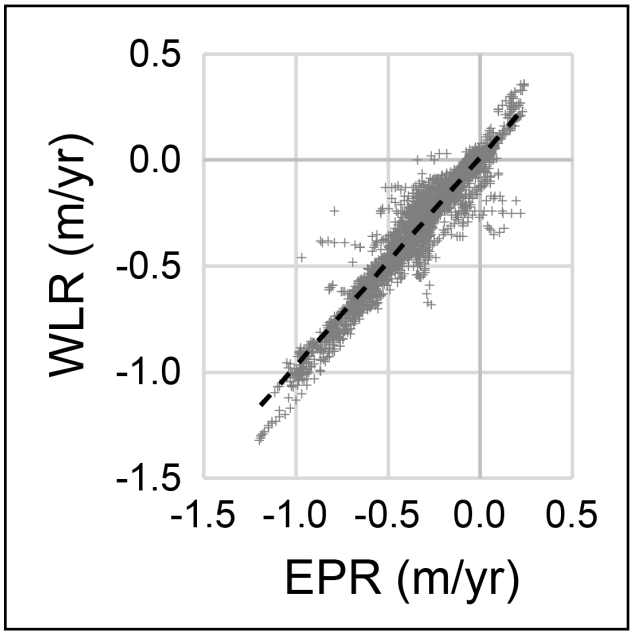

Figure 8. The end point rate (EPR) and weighted linear regression (WLR) shoreline change rate are highly correlated (slope = 0.99, R^2 = 0.92). EPR uses only the first and last shoreline. WLR uses all shorelines weighted by uncertainty.

area, Mount Augustine Drive, Bishop's Beach, the seawall at Munson Point, and various sections near East End Road. Historical erosion is relatively slow or stable in the Diamond Creek area and along the section of Kachemak Drive near the airport runway. Bluff toe erosion often outpaces bluff top edge erosion from the Bluff Point landslide area to Bishop's Beach, suggesting bluff steepening. The most significant toe erosion occurred after the 1964 earthquake (also observed by Stanley, 1968). Although this was a period of heightened erosion, it did not deviate significantly from the long-term change rate: the WLR rates of change are similar to EPR for both tops and toes (fig. 8). This finding suggests annualized erosion rates appropriately communicate erosion hazards in Homer, although erosion should not be expected on an annual basis. For example, if a shoreline eroded on average 3 ft/yr (1 m/yr), it may have remained stable for most of a 10-year period and eroded in one or a few episodes that total 30 ft (10 m).

Bluff Stability Assessment (Map Sheet 2: Coastal Bluff Stability)

Five variables are combined to visualize coastal bluff instability. Tall, steep bluffs with little vegetation, high drainage, rapid erosion, and no erosion protection have the highest hazard score. The area between the Bluff Point landslide and Bishop's Beach is found to be the least stable. Munson Point, where the seawall now exists, is generally the most stable in all categories except historical erosion.

DISCUSSION

This coastal hazard assessment covers historical shoreline change and current bluff stability. In this section, we summarize findings and observations by location, then discuss study limitations.

We break down results for six regions of Homer: Diamond Creek, Bluff Point Landslide Area, Downtown, Munson Point, Kachemak Drive, and East End Road (fig. 9; tables 11–13). Figures 10–12, 14, and 15 are screenshots from the oblique image-derived 3D model. This is a research tool to visualize the bluff complex for qualitative analysis, but many features and structures appear skewed due to insufficient overlap and camera angle.

Diamond Creek

The coastal bluffs of the Diamond Creek area reach from 250 to 500 ft (75 to 150 m) above MSL with an average slope of 17 ± 4 degrees (23 to 39 percent). They are typically exposed, with grass near the coast and denser vegetation on the flanks leading to a plateau above (fig. 10). Water seeps and surface water runoff are common. Much of the

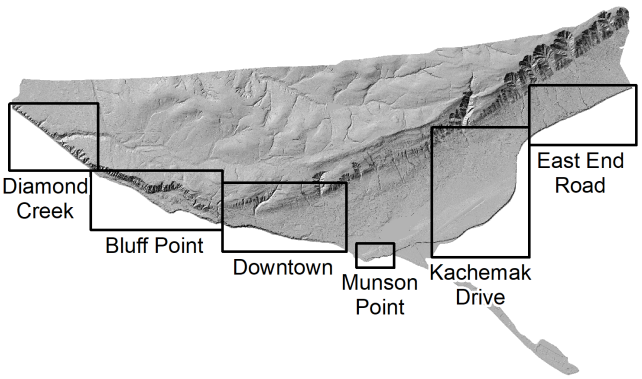

Figure 9. Discussion of results is divided into these six regions.

Table 13. Average coastal bluff instability by region. Scores range from 0 (very low instability) to 3 (high instability).

	Combined Instability	Combined Instability Score	Armor	Erosion	Slope	Veg.	Drainage
Diamond Crk	**Medium**	**1.8**	3.0	2.0	1.6	1.3	1.1
Bluff Pt	**Medium**	**2.0**	3.0	2.6	1.4	1.8	0.9
Downtown	**Medium**	**2.3**	3.0	2.7	2.0	2.4	0.7
Munson Pt	**Very Low**	**0.3**	1.2	1.4	0.8	1.8	0.3
Kachemak Dr	**Low**	**1.4**	2.8	1.7	1.3	1.5	0.4
East End Rd	**Medium**	**1.8**	3.0	2.8	0.8	1.9	0.7

Figure 10. Looking northeast at the coastal bluffs of Diamond Creek. The bluffs are tall, exposed, and undercut, leading to higher instability. This is a screenshot from our oblique image-derived 3D model.

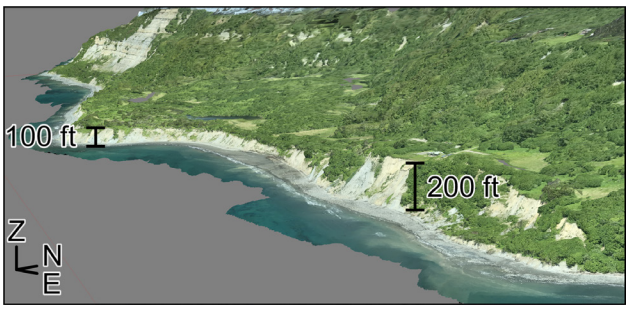

Figure 11. Looking northwest at the Bluff Point landslide area. The coastal bluffs are the seaward-most bluffs in this screenshot from our oblique image-derived 3D model. Unlike the larger bluffs in the background, these coastal bluffs are mostly unvegetated and experience significant erosion.

area has a low to medium bluff instability score, mainly due to fast erosion rates and high drainage.

Bluff Point Landslide Area

The Bluff Point landslide area is most notable for the tallest coastal relief in Homer, reaching up to 800 ft (240 m) above MSL. The lower landscape is formed from a widespread landslide deposit (Reger, 1979). The entire bluff complex is influenced by coastal processes over geologic timescales. Reger (1979) explains that the inland bluffs are relatively stable because wave action only reaches the landslide deposit, therefore we did not consider the larger landward bluffs to be coastal bluffs. The landslide deposit is so large that there are structures and small roads built upon it, and it has its own coastal bluffs about 30 to 100 ft (10 to 30 m) tall (fig. 11). These slopes are the second steepest in Homer, averaging 74 percent (36 degrees). This region has the fastest average erosion in Homer of -1.7 ft/yr (0.52 m/yr), reaching up to -3.7 ft/yr (-1.1 m/yr). The combined instability score of 2.0 (medium) is largely driven by these rapid erosion rates and the lack of vegetation on slopes. Despite steep slopes, the hazard due to slope failure is lower because they are relatively short (there is less inland erosion due to slope failure).

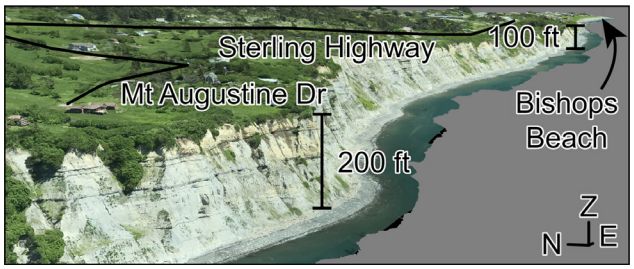

Figure 12. Looking east at the steep, exposed bluffs near Mount Augustine Drive in the oblique image-derived 3D model. The bluffs gradually shorten and become less steep toward Bishop's Beach.

Downtown

Coastal bluffs gradually transition from tall, steep, and exposed bluffs around Mount Augustine Drive to short and vegetated slopes at Bishop's Beach (fig. 12). This region has a high coastal bluff instability score due to tall, steep slopes, considerable erosion, and little to no vegetation. Even though the Bishop's Beach area has much lower bluffs, there are still hazards due to rapid erosion. In general, the exposed bluffs have greater erosion at the toe than the top, indicating bluff steepening. The greatest toe erosion occurred between 1951 and 1964, likely in the aftermath of the earthquake (Stanley, 1968).

Munson Point

Munson Point has very low coastal bluff instability due to relatively short slopes and a seawall (fig. 13). Before the seawall, this area had the fastest erosion in Homer (-3.9 ft/yr, -1.2 m/yr). The area received the lowest combined bluff instability score of all regions. This is due to the low bluffs, little drainage, and significant armoring preventing further erosion.

Kachemak Drive

The coastal bluffs along Kachemak Drive have low combined instability. There is relatively slow erosion to stable shorelines, and the area with the greatest erosion is now protected by gabion seawalls. The bluffs average 55 ft (17 m) tall with slopes around 35 degrees (73 percent). Some sections of the bluffs are densely vegetated, others exposed (fig. 14). No major streams run through this area. There are still some areas with medium to high instability due mainly to steepness, height, and lack of vegetation. Overall, this region has the second lowest instability score (table 13). Although erosion rates are slow, some structures are very close to the bluff edge.

East End Road

The bluffs near East End Road have medium instability. They average 68 ft (21 m) tall with an angle of 56 percent (29 degrees), which is low and shallow relative to western Homer. However, erosion rates average -1.1 ft/yr (-0.34 m/yr), the second fastest in Homer. There is no armoring and most bluffs have sparse vegetation or are bare. Drainage channels and groundwater seeps are common (fig. 15). These factors compound to elevate the instability score.

Study Limitations

This assessment is based on remotely sensed products and semi-automated techniques. This approach allows for a consistent metric to be

Figure 13. A. This 2019 photo looking northwest at Munson Point (left) shows the seawall protecting grassy and exposed bluffs. **B.** This closeup photo shows how water comes right up to the seawall and would surely undercut the bluffs.

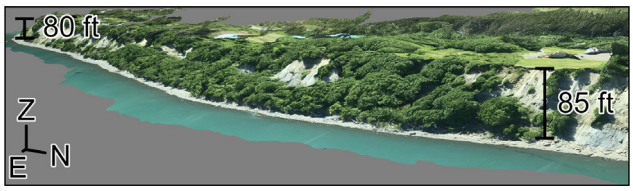

Figure 14. Looking west toward the partially vegetated bluffs near Kachemak Drive in the oblique image-derived 3D model.

Figure 15. Looking west toward the grassy-to-exposed bluffs and a densely vegetated creek near East End Road in the oblique image-derived 3D model. Exposed slopes show groundwater flow.

applied across broad scales, but it is less accurate at small scales because it is unsupervised. The results are appropriate for regional-scale assessments of hazards, but localized interpretations should be made with critical judgement.

Coastal bluffs can become destabilized by several compounding environmental factors (Hampton and Griggs, 2004). When deciding which bluff stability variables to include, we consider available data, relative influence of the variable, and whether it may be correlated with other data. For example, high winds erode bluffs, but the magnitude can be relatively small compared to erosion from wave action. Including wind as a parameter may have little to no influence on the results. In addition, by measuring observed shoreline change over decades, we summarize all major eroding forces. If we include specific drivers (such as wind or wave activity) as a separate variable from historical erosion, the two may be correlated enough to bias the combined instability score. Similarly, lithology is an important factor in bluff stability. Lithology influences slope, height, drainage, vegetation cover, and how quickly a bluff erodes. Homer's coastal bluffs have similar lithology throughout (sands, silts, and clays; Barnes and Cobb, 1959; Salisbury, in prep.). Due to the influence of lithology on so many variables and its homogeneity in the study area, we assume lithology is adequately represented. Ultimately, including the subtler influences on instability could improve this analysis, but they likely already factor into the existing variables.

Certain aspects of this study are automated; others are manually determined. We originally attempted an automated bluff top and toe detection using the method described by Palaseanu-Lovejoy and others (2016). The results were mostly accurate but required numerous minor fixes. Given the relatively small study area, it became faster and more accurate to delineate the bluff manually rather than correct the automated delineation. The U.S. Geological Survey (USGS) recently published the Cliff Feature Delineation Tool that also follows an automated method (Seymour and others, 2020). We tested the USGS tool on our dataset and found the results unfavorable. The processing tool we built proved most useful for analyzing slope, vegetation, and drainage statistics in a small area while allowing easy manual corrections using visual interpretations.

Shoreline change analyses have well-documented limitations related to data collection, analysis methods, and non-linear change drivers (Crowell and others, 2018; Overbeck and others, 2020). When using erosion rates, some important factors to consider are changes in drivers of erosion over time. Relative sea level fall (as is documented in Seldovia; NOAA CO-OPS, 2020b) can result in fewer wave impact hours, slowing erosion of the bluff toe. Changes in prevailing wind direction and intensity could change the wave climate, although only minor changes in winds have been measured in Homer (explore climate data at uaf-snap.org). Hydrographic changes, such as river channel migration or drainage infrastructure, can bring unprecedented change to an area. Engineered structures may age or be damaged, repaired, or newly installed, changing coastal dynamics in the immediate area as well as nearby coastlines (Rella and Miller, 2012).

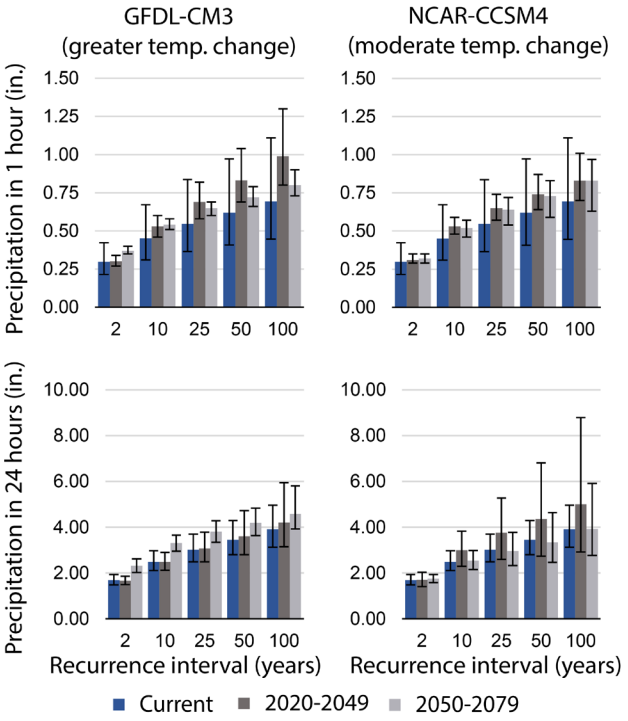

Figure 16. Current (blue) and future predicted (grayscale) precipitation trends in Homer, Alaska. The two columns show results from climate models predicting greater temperature change (left) and moderate temperature change (right). The rows show the current and predicted precipitation patterns in 1-hour (top) and 24-hour (bottom) periods. The Y axis is the total precipitation in inches. The X axis is the recurrence interval, from a 1- in 2-year event to a 1- in 100-year event. Modeled precipitation is similar to current conditions, especially considering the level of uncertainty. Data provided by uaf-snap.org.

These examples underscore the important considerations to make when using erosion rates.

Landslides can cause erosion outside the normal rate. Two major triggers for coastal bluff landslides are earthquakes and intense rainfall (Highland and Bobrowsky, 2008). Remarkably, the 1964 earthquake did not trigger major coastal landslides in Homer (Waller, 1966), but subsidence led to undercutting and swift erosion rates in the following years (Stanley, 1968). Climate model trends suggest a slight increase in extreme precipitation events in Homer, but there is no significant departure from current conditions (fig. 16). Regardless, current precipitation trends are enough to trigger landslides in Homer (Homer News, 2013). (See Salisbury [in prep.] for a full discussion on landslide susceptibility in Homer.)

Observations of 2009 Landslide in the Bluff Point Landslide Area

After completing this assessment, we found evidence that the 2009 landslide in the Bluff Point landslide area likely complicated erosion rates while providing insights into the connection between the coastal and inland bluffs. Between July 2 and July 3, 2009, two flanks collapsed in the Bluff Point landslide area and the beach uplifted as much as 15 ft (4.6 m), indicating a rotational slump occurred (Berg, 2009). Reger (1979) explains how these coastal bluffs are the eroded toes of rotated slump blocks from one or multiple ancient landslides. There are wide, underground shear planes connecting the inland bluffs to the coastal bluffs and beach (Berg, 2009). After a rotation, the uplifted area erodes. This process redistributes stress in the slump block back toward the bluff until another rotation occurs (fig. 2). The history of coastal erosion likely played a major role in destabilizing the bluff.

The 2009 landslide occurred across 800 ft (250 m) of shoreline, but comparisons of the 2008 and 2019 lidar reveal that the 2,500 ft (760 m) of coastal bluffs was translated seaward as far as 80 ft (25 m; fig. 17). The coastal bluffs remained mostly intact. Berg (2009) identified fissures in the slide mass that indicated active creeping. This suggests that the mass is debutressing from the inland bluff, leading to greater instability (B. Higman, written comm., 2021). Salisbury (in prep.) estimates that as far as 1,200 ft (366 m) inland from the bluff top edge is highly susceptible to a continued, retrogressive failure of the existing deep-seated rotational landslide block.

Where the Sterling Highway comes closest to the bluff edge (fig. 17, profile C), we did not find evidence of rotation from the 2009 landslide. The erosion history is similar to the nearby failure area, but the bluff is less steep. Continued erosion and bluff steepening decreases stability.

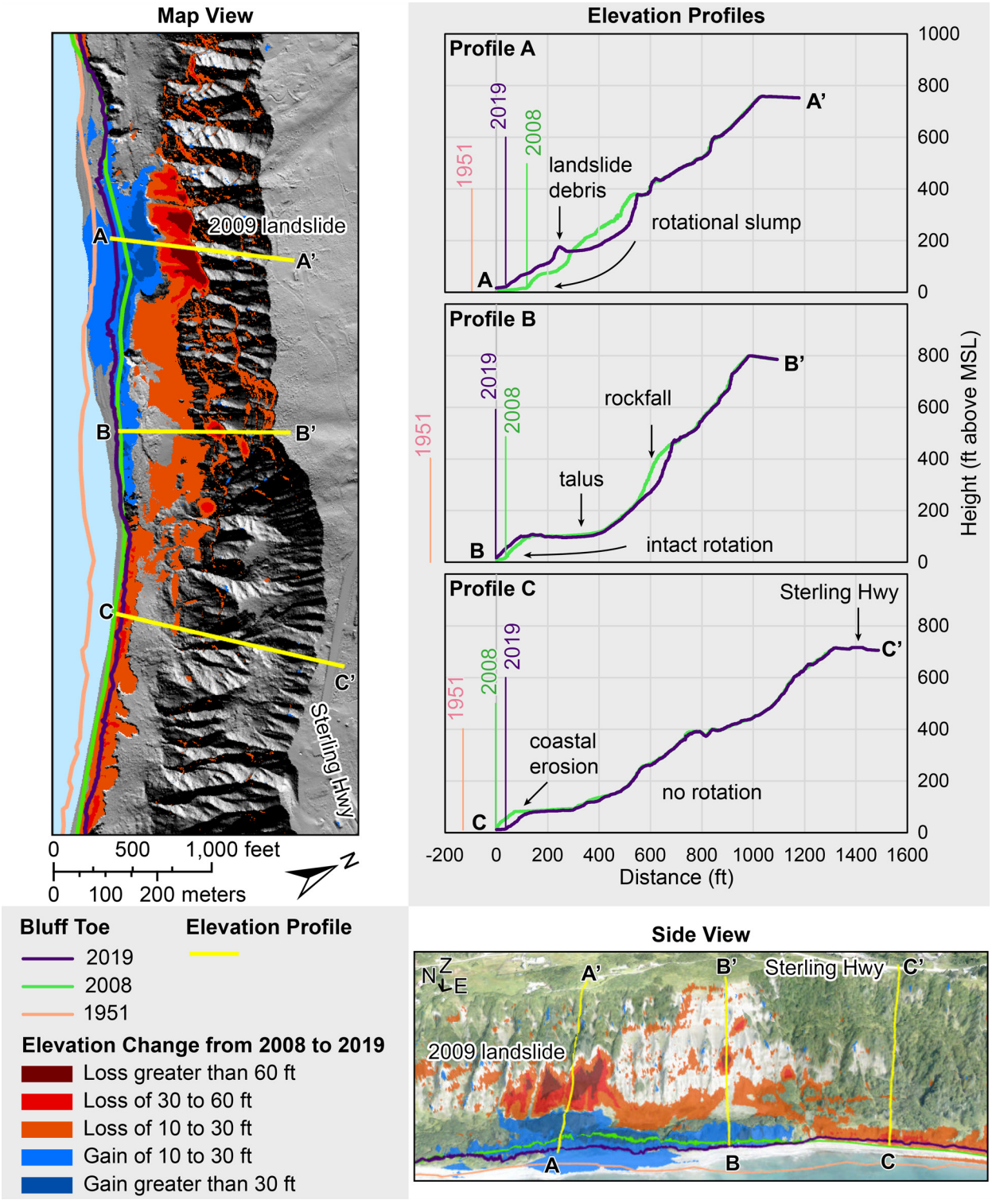

Figure 17. Map and side view of the region where the 2009 landslide occurred. The vertical change between the 2008 and 2019 lidar DTMs shows where the inland portion of the slump block lowered (warm colors) and rotated, uplifting the seaward section (cool colors). The bluff toe moved seaward between 2008 (green) and 2019 (purple). This is most apparent along profile A where the flank collapse occurred. On profile B, a smaller rockfall left a wide talus debris fan, and the coastal bluffs migrated seaward while remaining intact (carrying upright vegetation with them). Southeast of this area the rotation appears to end, and profile C has regular coastal erosion (also indicated by warm colors).

CONCLUSION

We assess coastal bluff stability for the Homer region using a shoreline change analysis and a combined coastal bluff instability score. Results indicate slow and ongoing erosion is steepening bluffs and encroaching on existing structures. Many bluffs have greater instability due to their height and slope, erosion at the toe, and lack of vegetation. The coastal bluff stability products highlight existing hazards and are tools to guide decisions to improve community safety.

ACKNOWLEDGMENTS

The Federal Emergency Management Agency (FEMA) provided funding through a Cooperative Agreement to the Alaska Division of Geological & Geophysical Surveys for the completion of this Coastal Bluff Stability Project under grant number EMS-2019-CA-00022-R05. We thank FEMA Cooperating Technical Partners Program, the City of Homer, and the Homer Planning Commission for supporting this work. Major improvements were made thanks to the thorough and insightful reviews by Bret "Hig" Higman, Chris Maio, Barrett Salisbury, and FEMA. Much of this study was possible thanks to the foundational work by Steve Baird and the Kachemak Bay National Estuarian Research Reserve.

REFERENCES

Ager, T.A., 1998, Postglacial vegetation history of the Kachemak Bay area, Cook Inlet, south-central Alaska, *in* Kelley, K.D., and Gough, L.P., eds., Geologic studies in Alaska by the U.S. Geological Survey, 1998: U.S. Geological Survey Professional Paper 1615, p. 147–165.

Baird, Steve, and Pegau, Scott, 2011, Coastal Change Analysis: Kachemak Bay Research Reserve, 18 p.

Barnes, F.F., and Cobb, E.H., 1959, Geology and coal resources of the Homer district, Kenai coal field, Alaska: U.S. Geological Survey Bulletin 1058-F, p. 217–260, 11 sheets.

Berg, Ed, 2009, Sudden uplift of the beach recalls ancient landslides: Kenai National Wildlife Refuge Notebook, v. 11, no. 27, p. 54–55.

Bishop, A.W., 1955, The use of the slip circle in the stability analysis of slopes: Géotechnique, v. 5, no. 1, p. 7–17.

Bukojemsky, Allegra, and Scheer, David, 2007, Stormwater and meltwater management and mitigation—A handbook for Homer, Alaska: DnA Design, 67 p.

Buzard, R.M., 2021, Photogrammetry-derived historical orthoimagery for Homer, Alaska from 1951, 1952, 1964, and 1985: Alaska Division of Geological & Geophysical Surveys Raw Data File 2021-21, 10 p. doi.org/10.14509/30824

Buzard, R.M., Maio, C.V., Verbyla, David, Kinsman, N.E.M., and Overbeck, J.R., 2020, Measuring historical flooding and erosion in Goodnews Bay using datasets commonly available to Alaska communities: Shore & Beach, v. 88, no. 3, p. 3–13.

Chowdhury, R.N., and Xu, D.W., 1994, Geotechnical system reliability of slopes: Reliability Engineering and System Safety, v. 47, p. 141–151.

City of Homer, 2021, Coastal erosion: City of Homer [website]: www.cityofhomer-ak.gov/planning/coastal-erosion

Crowell, Mark, Leatherman, S.P., and Buckley, M.K., 1991, Historical shoreline change—Error analysis and mapping accuracy: Journal of Coastal Research, v. 7, no. 3, p. 839–852.

Crowell, Mark, Leatherman, S.P., and Douglas, Bruce, 2018, Erosion—Historical analysis and forecasting, *in*, Finkl, C.W., and Makowski, C., eds., Encyclopedia of Coastal Science: Springer International Publishing AG, p. 428–432.

Gronewald, G.J., and Duncan, W.W., 1965, Study of erosion along Homer spit and vicinity, Kachemak Bay, Alaska, *in* Proceedings, Coastal Engineering Conference, American Society of Civil Engineers: New York, NY, p. 673–682.

Hales, T.C., and Miniat, C.F., 2017, Soil moisture causes dynamic adjustments to root reinforcement that reduce slope stability: Earth Surface Processes and Landforms, v. 42, no. 5, p. 803–813.

Hampton, M.A., and Griggs, G.B., 2004, Formation, evolution, and stability of coastal cliffs—status and trends: USGS Professional Paper 1693, 123 p.

Hapke, C.J., and Plant, N.G., 2010, Predicting coastal cliff erosion using a Bayesian probabilistic model: Marine Geology 278, p. 140–149.

Harp, E.L., Michael, J.A., and Laprade, W.T., 2006, Shallow-landslide hazard map of Seattle, Washington: U.S. Geological Survey Open-File Report 2006–1139, 18 p., 2 plates, map scale 1:25,000. pubs.usgs.gov/of/2006/1139/pdf/of06-1139_508.pdf

Heath, R.C., 1983, Basic ground-water hydrology: U.S. Geological Survey Water-Supply Paper 2220, 86 p.

Highland, L.M., and Bobrowsky, Peter, 2008, The landslide handbook—A guide to understanding landslides: Reston, Virginia, U.S. Geological Survey Circular 1325, 129 p.

Himmelstoss, E.A., Farris, A.S., Henderson, R.E., Kratzmann, M.G., Ergul, Ayhan, Zhang, Ouya, Zichichi, J.L., and Thieler, E.R., 2018, Digital Shoreline Analysis System (version 5.0): U.S. Geological Survey software release. code.usgs.gov/cch/dsas

Homer News, 2013, Heavy rains cause Homer mudslides: Homer News [website]: www.homernews.com/news/heavy-rains-cause-homer-mudslides/

Jiang, Shui-Hua, Huang, Jinsong, Yao, Chi, and Jianhua, Yang, 2017, Quantitative risk assessment of slope failure in 2-D spatially variable soils by limit equilibrium method: Applied Mathematical Modelling, v. 47, p. 710–725. dx.doi.org/10.1016/j.apm.2017.03.048

Kenai Peninsula Borough, 2019, Section 2.0—Floods and coastal erosion, *in* Hazard mitigation plan 2019 update: Kenai Peninsula Borough, 41 p.

———2021, Kenai Peninsula Borough GeoHub [website]: www.kpb.us/gis-dept

Kokutse, N.K., Temgoua, A.G.T., and Kavazović, Zanin, 2016, Slope stability and vegetation-conceptual and numerical investigation of mechanical effects: Ecological Engineering 86, p. 146–153.

Little, E.L., Jr., 1953, Check list of native and naturalized trees of the United States (including Alaska): U.S. Department of Agriculture, Agriculture Handbook 41, 472 p.

Maine Geological Survey, 2015, Coastal bluffs maps: Maine Geological Survey [website]: www.maine.gov/dacf/mgs/pubs/mapuse/series/descrip-bluff.htm

National Oceanic and Atmospheric Administration Center for Operational Oceanographic Products and Services (NOAA CO-OPS), 2020a, Coal Point, AK, [website]: tidesandcurrents.noaa.gov/datums.html?id=9455558

———2020b, Seldovia, AK, [website]: tidesandcurrents.noaa.gov/datums.html?id=9455500

Nilaweera, N.S., and Nutalaya, P., 1999, Role of tree roots in slope stabilisation: Bulletin of Engineering Geology and the Environment, v. 57, p. 337–342.

OCM Partners, 2021, 2019 USACE NCMP Topobathy Lidar—Alaska: NOAA [website]: www.fisheries.noaa.gov/inport/item/59331

Overbeck, J.R., Buzard, R.M., Turner, M.M., Miller, K.Y., and Glenn, R.J., 2020, Shoreline change at Alaska coastal communities: Alaska Division of Geological & Geophysical Surveys Report of Investigation 2020-10, 29 p., 45 sheets. doi.org/10.14509/30552

Palaseanu-Lovejoy, Monica, Danielson, Jeff, Thatcher, Cindy, Foxgrover, Amy, Barnard, Patrick, Brock, John, and Young, Adam, 2016, Automatic delineation of seacliff limits using lidar-derived high-resolution DEMs in Southern California, *in* Brock, J.C., Gesch, D.B., Parrish, C.E., Rogers, J.N., and Wright, C.W., eds., Advances in topobathymetric mapping, models, and applications: Journal of Coastal Research, Special Issue, no. 76, p. 162–173. doi.org/10.2112/SI76-014

Perello, Melanie, 2019, Draft Great Lakes coastal erosion—Review of erosion estimates, mapping, and public policies and outreach across the Great Lakes: Minnesota Department of Natural Resources, Lake Superior Coastal Program, 48 p. ardc.org/wp-content/uploads/2020/01/20191105_ReportOnGreatLakesErosionEfforts.pdf

Reger, R.D., 1979, Bluff Point landslide, a massive ancient rock failure near Homer, Alaska, *in* Short notes on Alaskan Geology, 1978: Alaska Division of Geological & Geophysical Surveys Geologic Report 61, p. 5–9.

Rella, A.J., and Miller, J.K., 2012, Engineered approaches for limiting erosion along sheltered shorelines—a review of existing methods: The Hudson River Sustainable Shorelines Project, 104 p. www.hrnerr.org/wp-content/uploads/sites/9/2012/07/limiteros.pdf

Ruggiero, Peter, 2010, Impacts of shoreline armoring on sediment dynamics, *in* Shipman, H., Dethier, M.N., Gelfenbaum, G., Fresh, K.L., and Dinicola, R.S., eds., 2010, Puget Sound shorelines and the impacts of armoring—Proceedings of a state of the science workshop, May 2009: U.S. Geological Survey Scientific Investigations Report 2010-5254, p. 179–186.

Salisbury, J.B., in prep., Landslide Susceptibility in Homer, Alaska: Alaska Division of Geological & Geophysical Surveys Report of Investigation.

Salisbury, J.B., Daanen, R.P., and Herbst, A.M., 2021, Lidar-derived elevation models for Homer, Alaska: Alaska Division of Geological & Geophysical Surveys Raw Data File 2021-2, 6 p. doi.org/10.14509/30591

Seymour, A.C., Hapke, C.J., and Warrick, Jonathan, 2020, Cliff feature delineation tool and baseline builder version 1.0 user guide: U.S. Geological Survey Open File Report 2020-1070, 54 p. doi.org/10.3133/ofr20201070

Stanley, K.W., 1968, Effects of the Alaska earthquake of March 27, 1964 on shore processes and beach morphology: Washington, DC, US Government Printing Office, 21 p.

U.S. Army Corps of Engineers (USACE), 2004, Low cost shore protection—a property owner's guide: Monroeville, Pennsylvania, GAI Consultants, Inc., 155 p.

Val, D.V., Yurchenko, Daniil, Nogal, Maria, and O'Connor, Alan, 2019, Chapter seven—Climate change-related risks and adaptation of interdependent infrastructure systems, *in* Bastidas-Arteaga, E., and Stewart, M.G., eds., Climate Adaptation Engineering: Butterworth-Heinemann, p. 207–242. doi.org/10.1016/C2017-0-00942-4

Varnes, D.J., 1978, Slope movement types and processes, *in* Schuster, R.L., and Krizek, R.J., eds., Landslides analysis and control: Washington, D.C., National Research Council, Transportation Research Board Special Report 176, p. 11–33. onlinepubs.trb.org/Onlinepubs/sr/sr176/176.pdf

Viereck, L.A., and Little, E.L., Jr., 1972, Alaska trees and shrubs, U.S. Department of Agriculture, Agriculture Handbook 410, 265 p.

Waller, R.M., 1966, Effects of the earthquake of March 27, 1964 in the Homer area, Alaska: U.S. Geological Survey Professional Paper 542-D, 28 p.

Winter, T.C., Harvey, J.W., Franke, L.O., and Alley, W.M., 1998, Ground water and surface water—A single resource: U.S. Geological Survey Circular 1139, 79 p.

Wu, T.H., 1984, Effect of vegetation on slope stability: Transportation Research Record, v. 965, p. 37–46.